Metrol. Meas. Syst., Vol. 30 (2023) No. 3, pp. 519–529
DOI: 10.24425/mms.2023.146417

PAN POLSKA AKADEMIA NAUK

METROLOGY AND MEASUREMENT SYSTEMS
Index 330930, ISSN 0860-8229
www.metrology.wat.edu.pl

M&MS

DETERMINATION OF ELECTRICAL AND THERMAL PARAMETERS OF VERTICAL-CAVITY SURFACE-EMITTING LASERS

Patrycja Śpiewak[1)], Marcin Gębski[1)], Włodek Strupiński[2,3)], Tomasz Czyszanowski[1)], Walery Kołkowski[2)], Iwona Pasternak[2,3)], Robert P. Sarzała[1)], Włodzimierz Nakwaski[1)], Michał Wasiak[1)]

1) Photonics Group, Institute of Physics, Lodz University of Technology, ul. Wólczańska 219, 90-924 Łódź, Poland (✉ *patrycja.spiewak@p.lodz.pl*)
2) Vigo Photonics S.A., ul. Poznańska 129/133, 05-850 Ożarów Mazowiecki, Poland
3) Faculty of Physics, Warsaw University of Technology, Koszykowa 75, 00-662 Warsaw, Poland

Abstract

Experimental methods are presented for determining the thermal resistance of vertical-cavity surface-emitting lasers (VCSELs) and the lateral electrical conductivity of their p-type semiconductor layers. A VCSEL structure was manufactured from III-As compounds on a gallium arsenide substrate. Conductivity was determined using transmission line measurement (TLM). Electrical and thermal parameters were determined for various ambient temperatures. The results could be used for computer analysis of VCSELs.

Keywords: TLM, thermal resistance, VCSEL, AlGaAs.

1. Introduction

Vertical-cavity surface-emitting lasers (VCSELs) are a specific type of semiconductor laser, in that output radiation is emitted from their surface. This enables emission of a relatively low-divergent circular output beam for a semiconductor laser. As a result, VCSEL lasers are an attractive option for creating two-dimensional arrays. Currently, commercial applications of VCSELs are mainly limited to devices emitting red or near infrared radiation. They are used to provide light sources for optical data transmission, optical mice, detection systems, smartphones, thermal material processing systems, proximity sensors, distance measurement systems, face recognition, Light Detection and Ranging (Lidar), and 3D printers [1–5]. These applications require VCSELs with strictly defined operating parameters, necessitating careful design. Therefore, it is important to know the different design and material parameters relevant to the operation of VCSELs. Computer simulations can be very helpful, making it possible to study the impact of various material and design parameters on, for example, output power and threshold current. Numerical methods

Article history: received March 2, 2023; revised April 12, 2023; accepted April 25, 2023; available online September 15, 2023.

are used to investigate many various interconnected physical phenomena occurring in VCSELs. They can also be used to separate and analyse a specific phenomenon, which is impossible with experimental methods. Moreover, using numerical methods can reduce the costs of manufacturing test structures. Unfortunately, not all of the values of material parameters necessary for numerical analysis have been measured precisely. Others may vary, depending on the fabricating system. Some, such as the resistance of electrical contacts, are mostly dependent on the technology used.

In this study, TLM measurements [9–11] were used to determine the electrical parameters of a VCSEL. The quality of the electrical contacts, especially the p-side contacts, has a significant impact on the performance of VCSELs. Equally important are the thermal properties of VCSELs because they influence the laser performance. In general, the thermal properties of a device are described in terms of thermal resistance. A low value for thermal resistance allows for more efficient operation. Therefore, thermal resistance was also measured, using a method similar to that described in [12]. A slightly different method of determining this parameter can be found in [13]. In future work, the electrical and thermal parameters determined here will be used in computer simulations of VCSELs.

2. Determination of lateral electrical conductivity

The VCSELs used in this study were produced by Vigo Photonics. The VCSELs were manufactured as GaAs/AlGaAs structures. Their top *distributed Bragg reflectors* (DBRs) are composed of 18 pairs of alternate layers of $Al_{0.9}Ga_{0.1}As$ and $Al_{0.2}Ga_{0.8}As$ of thicknesses approximately equal to a quarter of the emission wavelength each. The DBR layers are separated by thin gradient layers of compositions linearly changing from $Al_{0.9}Ga_{0.1}As$ to $Al_{0.2}Ga_{0.8}As$ or inversely. The VCSEL semiconductor structures are terminated on both sides by thin highly-doped GaAs layers, on which Ti/Pt/Au contacts are deposited. This structure is described in detail in [14].

Semiconductor samples with metallic contacts were submitted to *transmission line measurement* (TLM) (Fig. 1). This method was used to determine two electrical parameters important from the point of view of VCSEL operation:

1) surface resistivity of the metal–semiconductor contact,
2) lateral electrical conductivity of the semiconductor area below the contacts.

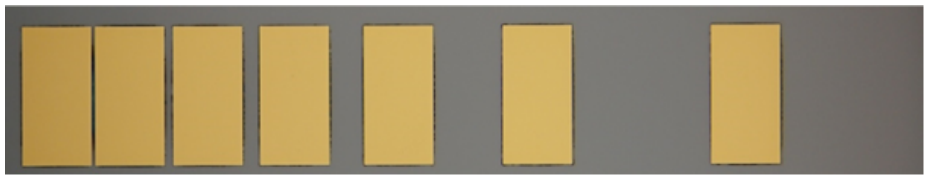

Fig. 1. Exemplary photographs of TLM samples produced by Vigo Photonics.

The TLM method consists in determining the resistance between adjacent contacts. In our measurement arrangement, the contacts were connected with the poles of a supply system by needles (Fig. 2 and Fig. 3). The current flowed from the first needle through the gold pad, then through the semiconductor area below, and finally reached the pad to which the second needle was connected (Fig. 2). Vertical current spreading was limited by the p–n junction, which presented a barrier to the current.

TLM measurements were carried out by the Photonics Group at Lodz University of Technology. During the measurements, current-voltage dependence was recorded, from which resistance

Metrol. Meas. Syst., Vol. 30 (2023), No. 3, pp. 519–529
DOI: 10.24425/mms.2023.146417

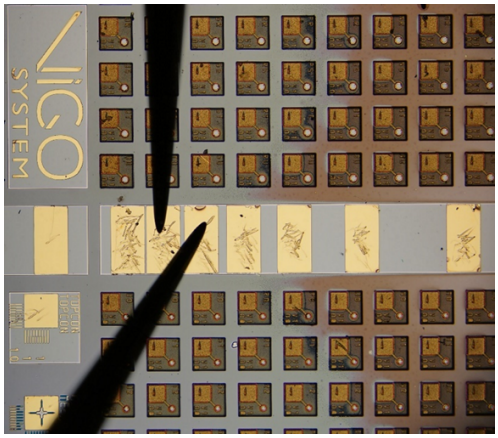

Fig. 2. Photograph of measured TLM samples produced by Vigo Photonics.

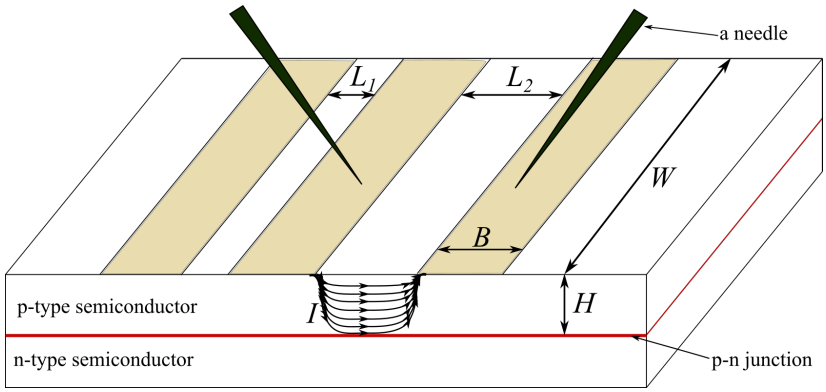

Fig. 3. Scheme of the TLM measurement with current paths between the contacts indicated: L – distance between the contacts; W – width of the contacts; H – thickness of semiconductor layers conducting the current.

was determined. Device resistance is the sum of the contact resistances and the semiconductor resistance [15]. Measurements were carried out for various distances L between two contacts of the same width $W = 400$ µm (Fig. 3). Distances L were between 10 µm and 3200 µm. In general, the sample dimensions should meet the following dependence:

$$W \gg L \gg H, \tag{1}$$

where H is the thickness of the semiconductor layer below the contact. Dependence $R(L)$ is approximately linear and its slope coefficient α can be expressed as [16]:

$$\alpha = \frac{R_{\mathrm{sh}}}{W} = \frac{1}{\sigma_p \cdot H \cdot W}, \tag{2}$$

where R_{sh} is the sheet resistance of the semiconductor layer below the contacts, σ_p is the effective electrical conductivity in the lateral direction of that layer, and H its thickness.

The condition $W \gg L$ in relation (1) is necessary to assume homogeneous current spreading for the whole width of the contact. Our sample does not satisfy this condition (see Fig. 2), but

a homogeneous current flow is still fulfilled as a result of etching the lateral areas to the depth below the p–n junction, which creates the mesa structure. In general, most VCSELs consist of alternately arranged thin layers of semiconductors, which form two DBRs located on either side of the junction. A detailed description of the analysed structures can be found in Section 2.2.

The standard formulas used in the analysis of TLM measurements are derived with the following essential and generally not always true assumptions:

1. The thickness H of a layer conducting current is sufficiently low to assume a homogeneous current flow within the layer.
2. Electrical contacts are semi-infinite in the direction of current flow ($B = \infty$ – see Fig. 3).
3. Contact resistance is identical for both possible directions of the current flow through the metal-semiconductor contact.

The second assumption can be verified by determining the parameters with the aid of standard formulas. The current distribution along the direction of the current flow below the contact disappears exponentially as a function of the distance from the contact edge [16]. Hence, inaccuracy r following the second condition may be estimated as the ratio of the amount of current flowing through the real width of the contact (B) to the total current, both calculated using approximation (2). A simple integration gives:

$$r = \exp\left(-B\sqrt{\frac{\sigma_c}{H \cdot \sigma_p}}\right), \tag{3}$$

where H is thickness of the semiconductor area below the contacts, σ_p is the effective electrical conductivity of the semiconductor material, and σ_c is the electrical conductivity of the contacts. Parameter r in relation (3) describes the relative difference between the contact resistance of width B and a semi-infinite contact. Therefore, the contacts should be larger if the conductivity of the semiconductor material or its thickness increases, as well as when the conductivity of the contacts is worse. For the measurements presented in this paper, relation (3) leads to $r = 1.8 \cdot 10^{-11}$, which we consider to be a sufficiently low value.

It is impossible to verify the authenticity of the third assumption if the two contacts are identical, as they are in our case. Hence, we determine the average value for conductivity in two current-flow directions, up and down. When concentric annular contacts are used instead of perpendicular contacts, theoretical analysis becomes much more complex and analysis of measurement results is more difficult.

Figure 4 presents schemes of the structure with and without an etched mesa. The etching on the lateral areas enables measurements for larger ranges of the L parameter, which increases the accuracy with which the conductivity of the semiconductor layer can be determined, especially at higher values. Figure 5 presents resistance R of the area between adjacent contacts as a function

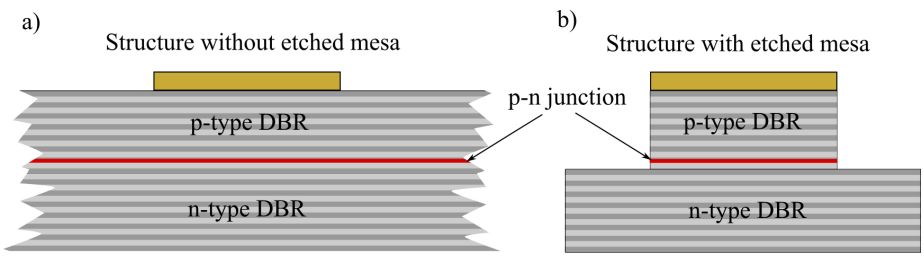

Fig. 4. Scheme of two types of structure submitted to TLM measurements: a) without an etched mesa, b) with an etched mesa.

Metrol. Meas. Syst., Vol. 30 (2023), No. 3, pp. 519–529
DOI: 10.24425/mms.2023.146417

of the distance between the contacts. It shows that mesa etching allows a linear $R(L)$ dependence to be obtained for significantly large values of the L parameter. This is especially important for measuring well-conducting semiconductors, for example, n-type semiconductors.

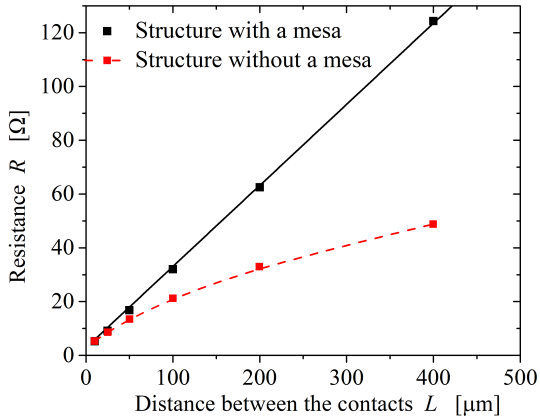

Fig. 5. Exemplary plots of the resistance R as a function of the distance between adjacent contacts for two structures: with a mesa and without a mesa.

Formula (2) was used to determine the conductivities of the semiconductor layers below the contacts at various heat-sink temperatures between 20°C and 80°C. The measurements were carried out for two contact structures, denoted here as TLM 1 and TLM 2. As an example, the current-voltage characteristic is presented in Fig. 6 for the TLM 1 sample at 20°C. The lateral electrical conductivity was about 3300/(Ωm) at 20°C and gradually fell as temperature increased to about 2800–2900/(Ωm) (Fig. 7). The calculations carried out for the TLM 1 sample show lower conductivities, because it was situated closer to an edge of the sample slab than the TLM 2 sample. The thickness of epitaxial layers (H parameter) is sometimes a little lower near to the sample edge than in the centre, which, following Formula (2), leads to lower calculated electrical conductivity.

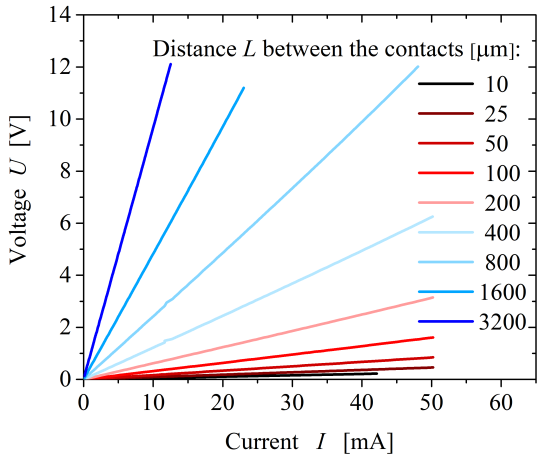

Fig. 6. Current-voltage characteristics at 20°C for the TLM 1 sample and for various distances L between the contacts.

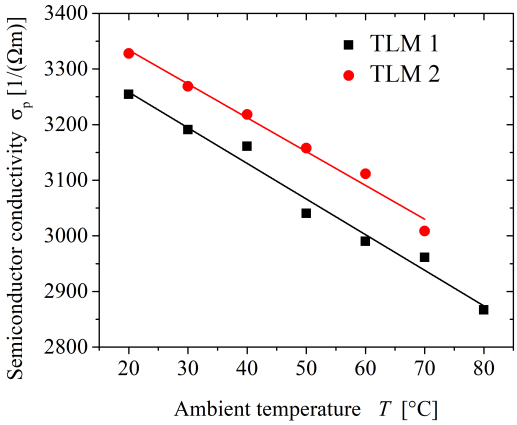

Fig. 7. Temperature dependence of the effective lateral electrical conductivity σ_P of the p-type semiconductor layers for two samples: TLM 1 and TLM 2.

The experimental values for contact resistance were in the range of $2 \cdot 10^{-5}$ Ωcm^2–$1 \cdot 10^{-4}$ Ωcm^2 for temperatures between 20°C and 80°C. The average value of the slope coefficients of both the $\sigma_p(T)$ relations shown in Fig. 7 is – 6.24/(ΩmK). Contact conductivity was sufficiently high to assume that the resistance of the p-side contact was negligible compared to the device resistance. The cup layer (subcontact layer) on the p-side of the analysed laser was doped with Zn+ ions at the level of $1.2 \cdot 10^{20}$ cm^{-3}. According to data from [17], the conductivity of p-type contacts doped with C+ ions of $1 \cdot 10^{20}$ cm^{-3} is $7 \cdot 10^{-6}$ Ωcm^2.

3. Determination of thermal resistance

In the second part of the study, we investigated the thermal resistance R_{th} of the VCSELs as a function of various heat-sink temperatures, based on measurements of its *light-current-voltage* (LIV) characteristics. Emission spectra were also recorded, using a Yokogawa AQ6370D Optical Spectrum Analyzer. Thermal resistance can be defined as a derivative of the laser temperature in the active area T_j over dissipated power P_{diss}:

$$R_{\text{th}} = \frac{\mathrm{d}T_j}{\mathrm{d}P_{\text{diss}}}, \tag{4}$$

where T_j is the temperature of the active-region and $P_{\text{diss}} = U \cdot I - P_{\text{out}}$, where P_{out} is the optical output power. The spectrum shift towards longer wavelengths (so called red shift) is caused by the increase of temperature in the active areas. The temperature of the laser can be raised by the flow of electric current through the laser or by the heating of its heat-sink. In the first case, changing the wavelength involves different mechanisms of power dissipation. On the other hand, the laser temperature depends on the power emitted by the device. Therefore, the following formula is correct:

$$\lambda(P_{\text{diss}}) = \lambda(T_j(P_{\text{diss}})). \tag{5}$$

After counting the derivative of relation (4), we obtain the following formula:

$$\frac{\mathrm{d}\lambda}{\mathrm{d}P_{\text{diss}}} = \frac{\mathrm{d}\lambda}{\mathrm{d}T_j} \cdot \frac{\mathrm{d}T_j}{\mathrm{d}P_{\text{diss}}}. \tag{6}$$

Metrol. Meas. Syst., Vol. 30 (2023), No. 3, pp. 519–529
DOI: 10.24425/mms.2023.146417

Using (4) and (6), the formula for thermal resistance can be presented using wavelength λ [5]:

$$R_{\text{th}} = \frac{\mathrm{d}T_j}{\mathrm{d}\lambda} \cdot \frac{\mathrm{d}\lambda}{\mathrm{d}P_{\text{diss}}} . \tag{7}$$

Two experiments were performed to determine the R_{th}. Each experiment was performed separately to determine the two components of the product of (7).

First, the laser spectra for the different temperatures of the heat sink T_{amb} were measured for a current value slightly above the threshold current to minimize the heating of the laser due to the current flow. Assuming a constant or low value for the current flowing through the laser, the wavelength shift is due to the change in the laser temperature caused by a change in the temperature of the heat-sink. Then, measuring the laser spectra enables determination of wavelengths corresponding to the highest emission peaks (Fig. 8), from which the slope $\mathrm{d}T_{\text{amb}}/\mathrm{d}\lambda$ of the $T_{\text{amb}}(\lambda)$ curve is determined. In our assumptions, this slope coefficient is equivalent to the $\mathrm{d}T_j/\mathrm{d}\lambda$. The measurements were carried out for constant temperatures of the heat-sink from 25°C to 85°C.

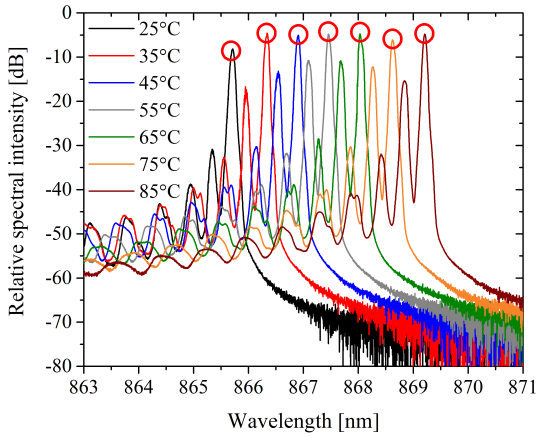

Fig. 8. VCSEL spectra determined for various heat-sink temperatures and currents slightly exceeding their lasing thresholds. The peaks corresponding to the longest wavelengths are marked by circles.

The second factor in (7), $\mathrm{d}\lambda/\mathrm{d}P_{\text{diss}}$, describes the changes in the laser's wavelength caused by the increase in power dissipated in the device. It was determined from spectra measured at a constant temperature of the heat sink, but for different values of the driving current. Figure 9b presents the LIV characteristics at 25°C for three currents, 5 mA, 9 mA, and 12 mA. As can be seen, the main peak is shifted towards longer wavelengths as the current increases. Figure 10 shows the wavelength of the peak as a function of dissipated power $\lambda(P_{\text{diss}})$ for different temperatures of the heat-sink.

Dependence $\lambda(P_{\text{diss}})$ is approximately linear and enables determination of the $\mathrm{d}\lambda/\mathrm{d}P_{\text{diss}}$ value. As a consequence, the thermal resistance of the VCSEL can be determined using Formula (7). This procedure was applied for ambient temperatures T_{amb} within the range of 25–85°C, which showed the dependence of the thermal resistance on temperature $R_{\text{th}}(T)$ (Fig. 11).

For the investigated VCSEL at room temperature, the thermal resistance was equal to 1.87 K/mW. The thermal resistance depends on the electrical aperture of the laser and increases as the aperture size decreases. The analysed VCSEL has an electrical aperture of about 5 µm.

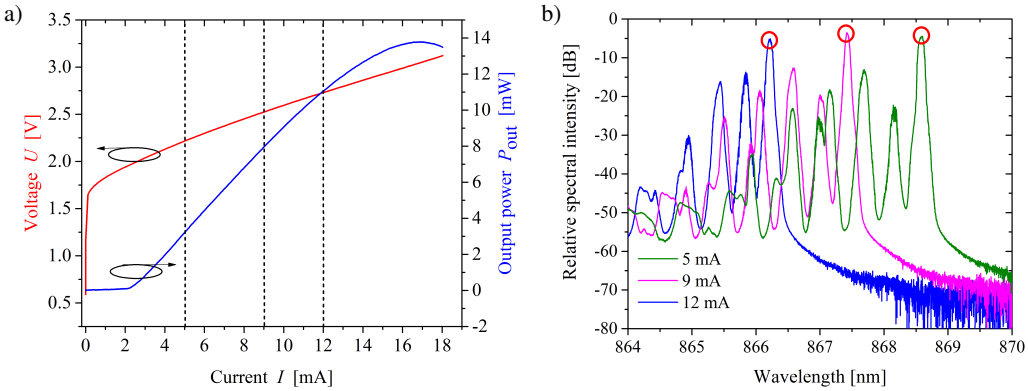

Fig. 9. Light-current-voltage (LIV) (a) and emission spectra (b) of the considered VCSEL at the ambient temperature of 25°C. Emission spectra (b) were recorded for three selected currents. Dashed lines in (a) indicate the currents for which red circles in (b) signify spectral peaks.

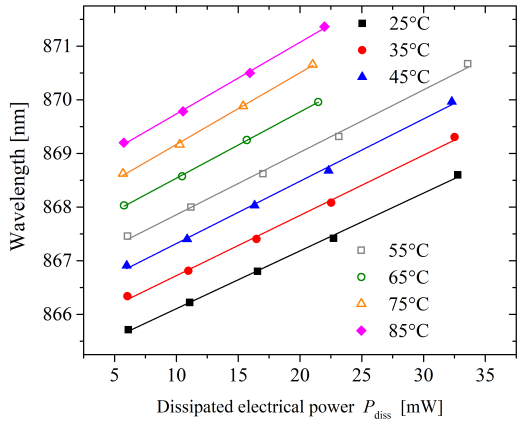

Fig. 10. Wavelength as a function of the dissipated power P_{diss} for the analysed VCSEL.

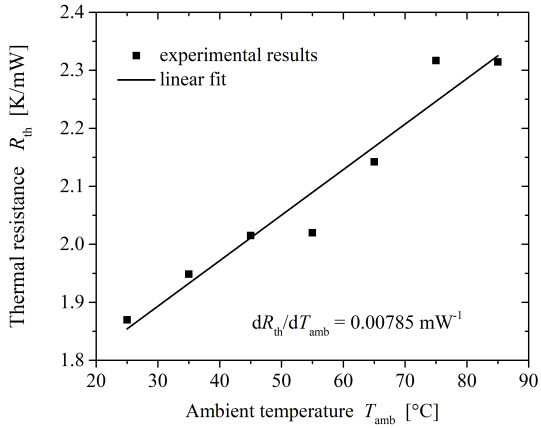

Fig. 11. Thermal resistance of the considered VCSEL as a function of temperature.

Metrol. Meas. Syst., Vol. 30 (2023), No. 3, pp. 519–529
DOI: 10.24425/mms.2023.146417

According to the literature data, VCSELs produced from arsenide material with similar apertures have thermal resistances in the range 0.5–2.8 K/mW [18–20]. Therefore, we can conclude that the analysed laser has good, relatively low thermal resistance.

4. Conclusions

In this study, a modified TLM method was used to characterize the parameters of VCSELs. We modified the standard TLM layout by etching a mesa which prevents the current from spreading outwards. This modification allowed us to use distances between the electrodes much bigger than their width which increases the accuracy of the measurement, especially when the conductivity of the semiconductor is high. The surface conductivity of the contacts and the conductivity of the semiconductor material were typical for p-type AlGaAs. The tested VCSELs were also found to have good thermal parameters, with low thermal resistance. The method described here enables measurements with larger distances between the VCSEL contacts, which improves their accuracy. This can be especially important in the samples where the semiconductor material has high conductivity. In future work, the determined electrical and thermal parameters will be used in computer simulations of VCSELs.

Acknowledgements

The authors would like to thank the National Centre for Research and Development for supporting research and development of VCSELs technology within the MAZOWSZE/0032/19-00 grant.

References

[1] Iga, K. (2008). Vertical-cavity surface-emitting laser: Its conception and evolution. *Japanese Journal of Applied Physics*, *47*(1R), 1. https://doi.org/10.1143/JJAP.47.1

[2] Koyama, F. (2006). Recent advances of VCSEL photonics. *Journal of Lightwave Technology*, *24*(12), 4502–4513. https://doi.org/10.1109/JLT.2006.886064

[3] Li, X., Liu, C., Wang, Z., Xie, X., Li, D., & Xu, L. (2020). Airborne LiDAR: state-of-the-art of system design, technology and application. *Measurement Science and Technology*, *32*(3), 032002. https://doi.org/10.1088/1361-6501/abc867

[4] Dobosz, M. (2012). Laser diode distance measuring interferometer-metrological properties. *Metrology and Measurement Systems*, *19*(3), 553–564. https://doi.org/10.2478/v10178-012-0048-1

[5] Chen, B., Claus, D., Russ, D., & Nizami, M. R. (2020). Generation of a high-resolution 3D-printed freeform collimator for VCSEL-based 3D-depth sensing. *Optics Letters*, *45*(19), 5583–5586. https://doi.org/10.1364/OL.401160

[6] Gębski, M., Wong, P. S., Riaziat, M., & Lott, J. A. (2020). 30 GHz bandwidth temperature stable 980 nm VCSELs with AlAs/GaAs bottom DBRs for optical data communication. *J. Phys. Photonics*, *2*(3), 035008. https://doi.org/10.1088/2515-7647/ab9420

[7] Okur, S., Scheller, M., Seurin, J. F., Miglo, A., Xu, G., Guo, D., ... & Ghosh, C. (2019, March). High-power VCSEL arrays with customized beam divergence for 3D-sensing applications. In *Vertical-Cavity Surface-Emitting Lasers XXIII* (Vol. 10938, pp. 61–67). SPIE. https://doi.org/10.1117/12.2508485

[8] Fujioka, I., Ho, Z., Gu, X., & Koyama, F. (2020, May). Solid state LiDAR with sensing distance of over 40m using a VCSEL beam scanner. In *CLEO: Science and Innovations* (pp. SM2M-4). Optical Society of America. https://doi.org/10.1364/CLEO_SI.2020.SM2M.4

[9] Reeves, G. K., & Harrison, H. B. (1982). Obtaining the specific contact resistance from transmission line model measurements. *IEEE Electron Device Letters*, *3*(5), 111–113. https://doi.org/10.1109/EDL.1982.25502

[10] Baca, A. G., Ren, F., Zolper, J. C., Briggs, R. D., & Pearton, S. J. (1997). A survey of ohmic contacts to III-V compound semiconductors. *Thin Solid Films*, *308*, 599–606. https://doi.org/10.1016/S0040-6090(97)00439-2

[11] Lyu, Y. T., Jaw, K. L., Lee, C. T., Tsai, C. D., Lin, Y. J., & Cherng, Y. T. (2000). Ohmic performance comparison for Ti/Ni/Au and Ti/Pt/Au on InAs/graded InGaAs/GaAs layers. *Materials Chemistry and Physics*, *63*(2), 122–126. https://doi.org/10.1016/S0254-0584(99)00208-4

[12] Daubenschüz, M., & Michalzik, R. (2016, April). Parameter extraction from temperature-dependent light-current-voltage data of vertical-cavity surface-emitting lasers. In *Semiconductor Lasers and Laser Dynamics VII* (Vol. 9892, pp. 115–122). SPIE. https://doi.org/10.1117/12.2228080

[13] Flick, T., Becks, K. H., Dopke, J., Mättig, P., & Tepel, P. (2011). Measurement of the thermal resistance of VCSEL devices. *Journal of Instrumentation*, *6*(01), C01021. https://doi.org/10.1088/1748-0221/6/01/C01021

[14] Gębski, M., Śpiewak, P., Kołkowski, W., Pasternak, I., Głowadzka, W., Nakwaski, W., ... & Strupiński, W. (2021). First vertical-cavity surface-emitting laser made entirely in Poland. *Bulletin of the Polish Academy of Sciences: Technical Sciences*, e137272–e137272. https://doi.org/10.24425/bpasts.2021.137272

[15] Gary Tuttle, "Contact resistance and TLM measurements" Dept. of Electrical and Computer Engineering, Iowa State University. https://gtuttle.net/fabrication/topics/tlm_measurements.pdf

[16] Schroder, D. K. (2015). *Semiconductor Material and Device Characterization*. John Wiley & Sons, Ch. 1 Resistivity, pp. 138-143.

[17] Katz, A., Abernathy, C. R., & Pearton, S. J. (1990). Pt/Ti ohmic contacts to ultrahigh carbon-doped p-GaAs formed by rapid thermal processing. *Applied Physics Letters*, *56*(11), 1028–1030. https://doi.org/10.1063/1.102605

[18] Mimura, M., & Miyamoto, T. (2018). Thermal conductivity reduction effect of thin layer on thermal resistance of vertical cavity surface emitting lasers. *Japanese Journal of Applied Physics*, *57*(8S2), 08PD02. https://doi.org/10.7567/JJAP.57.08PD02

[19] Al-Omari, A. N., Carey, G. P., Hallstein, S., Watson, J. P., Dang, G., & Lear, K. L. (2006). Low thermal resistance high-speed top-emitting 980-nm VCSELs. *IEEE Photonics Technology Letters*, *18*(11), 1225–1227. https://doi.org/10.1109/LPT.2006.875059

[20] Liao, W. Y., Li, J., Li, C. C., Guo, X. F., Guo, W. T., Liu, W. H., ... & Tan, M. Q. (2020). Oxide-aperture-dependent output characteristics of circularly symmetric VCSEL structure. *Chinese Physics B*, *29*(2), 024201. https://doi.org/10.1088/1674-1056/ab5fbd

Metrol. Meas. Syst., Vol. 30 (2023), No. 3, pp. 519–529
DOI: 10.24425/mms.2023.146417

Patrycja Śpiewak received her M.Sc. Ph. D. degrees, both in physics, from the Lodz University of Technology, Łódź, Poland, in 2015 and 2022 respectively. She is currently with the Photonics Group, Lodz University of Technology. Her research interests include computer modelling of arsenide and nitriside VCSELs and experimental characterization of semiconductor lasers.

Marcin Gębski received his M.Sc. degree in physics from the Lodz University of Technology, Poland in 2012 on the subject of numerical simulations of the highly strained dilute nitride multi-step QWs for vertical-cavity surface-emitting lasers (VCSELs) emitting in NIR for telecommunication applications. He received his PhD in physics from the same university in 2017 on the subject of VCSELs incorporating monolithic high-contrast grating (MHCG) mirrors. He presented the world's first electrically-injected MHCG VCSEL in 2019 and is one of the developers of the VCSEL technology in Poland. His current research interests include investigating optical properties of VCSEL lasers and MHCG microcavities and developing fabrication technology of semiconductor lasers.

Włodek Strupiński is head of the Epitaxy Department at Vigo Photonics, being responsible for the development and fabrication of various III–V compound semiconductor heterostructures for photonics and microelectronics. He has had more than 30 years' experience in III–V technology, specializing in vapor phase epitaxy and metalorganic vapor phase epitaxy of GaAs-, InP-, GaN-related, SiC as well as in graphene and other 2D nanomaterials. Before joining Vigo he had worked at ITME (Institute of Electronic Materials Technology) where he developed many epitaxial technologies later successfully used in experimental or commercial production.

Walery Kołkowski, completed his Ph.D. thesis in semiconductor physics at the Institute of Physics, Polish Academy of Sciences. His research there focused on the growth of thin II-VI semiconductor structures and nanostructures by molecular beam epitaxy (MBE). After receiving his doctorate, Kołkowski moved to Germany in 2017 to work as a postdoc at the Technische Universität, Dresden. In 2019, he joined VIGO Photonics as a senior engineer in the Epitaxy Department. In this role, he focuses on the MOCVD growth of novel semiconductor structures, integration of dissimilar materials, and strained thin-film heterostructures.

Tomasz Czyszanowski received his M.Sc. and Ph.D. degrees in physics from the Lodz University of Technology, Poland, in 2000 and 2004 respectively, and D.Sc. degree in physics from the Wroclaw University of Technology, Poland, in 2012. In 2019 he become a full professor. After receiving his M.Sc., he was a visiting researcher at CFD Research Corporation, Huntsville, Alabama, where he worked mainly on optical scalar models of semiconductor lasers. His Ph.D. work involved studies on the validity limits of optical models used in simulations of semiconductor lasers. From 2005 to 2007 he was a post-doctoral researcher at Vrije University, Brussels, Belgium, on a fellowship awarded by the Foundation for Polish Science. There he analysed the performance of photonic-crystal VCSELs. In 2012 he was appointed Associate Professor at the Institute of Physics at the Lodz University of Technology, Poland. The current area of research of his research team and himself involves the modelling GaAs-, GaN-, InP- based VCSELs, modelling, processing and characterization of irregular and coupled-cavity VCSELs, modelling of resonant, reflective and transparent subwavelength periodic structures.

Iwona Pasternak received her PhD in Materials Engineering. She is an expert in the Epitaxy Department at VIGO System SA. She also cooperates with the Faculty of Physics of Warsaw University of Technology (WUT) where she develops the graphene and other 2D materials growth technology. At VIGO she focuses on characterization and manufacturing of epitaxial structures of III–V semiconducting compounds.

Włodzimierz Nakwaski (IEEE M'96–SM'03) received the M.Sc. (cum laude) degree in electrical engineering from the Lodz University of Technology, Łódź, Poland, in 1971, the M.Sc. degree in physics from Lodz University, Łódź, in 1973, and the Ph.D. (cum laude) and D.Sc. degrees in electrical engineering from the Institute of Electron Technology, Warsaw, Poland, in 1976 and 1985, respectively. In 1996, he received the scientific title of Professor in Physics. In 1974, he joined the Institute of Electron Technology, Warsaw, where he was involved in theoretical and experimental investigations of diode lasers and LEDs. He has been with the Lodz University of Technology since 1975, as a Full Professor since 1999. In 1990, he joined the University of New Mexico, Albuquerque, NM, USA, initially as a Visiting Senior Research Scientist. Since1993, he has been an Adjunct Associate Professor with the University of New Mexico. He holds five patents and has authored or co-authored over 500 technical papers and conference contributions, three books, and seven chapters in books. His current research interests include modelling physical phenomena occurring in optoelectronic devices, in particular computer simulation of the operation of various types of diode laser, including VCSELs, taking into consideration the mutual interactions between thermal, optical, electrical, recombination, and mechanical phenomena, to assist in their design and optimization.

Robert Sarzała, associate professor, has been working at the Lodz University of Technology since 1990. He obtained a Ph.D. degree in electronics from the Institute of Electronic Technology in Warsaw in 1998. In June 2005, he passed the habilitation colloquium before the Scientific Council of the Institute of Physics at the Wroclaw University of Technology, obtaining the degree of habilitated doctor in physical sciences in the discipline of physics. He is a specialist in solid-state physics, particularly in optoelectronics. His research interests include the development of advanced models and computer programs enabling comprehensive analysis of physical phenomena occurring during the operation of semiconductor lasers, particularly VCSEL lasers and their two-dimensional arrays. Throughout his professional career, he has also conducted research on edge emitting lasers and their arrays, QCL lasers, and VECSEL lasers. Thermal phenomena occurring during the operation of various types of semiconductor lasers are of particular importance in his previous research. He is a co-author of over 450 scientific publications, 6 chapters in scientific books, 4 national monographs, and 6 patent applications. For his scientific and innovative activities, he has been awarded 9 international prizes and 3 awards from the Minister of National Education. He has supervised 4 Ph.D. students.

Michał Wasiak received the Ph.D. degree in physics from the Lodz University of Technology, Łódź, Poland, in 2004, and the D.Sc. degree from the Institute of Physics, Polish Academy of Sciences, in 2018. He is currently with the Institute of Physics, Lodz University of Technology. His current research interests include modelling modulation properties of blue and NIR VCSEL lasers and experimental investigations of material and device properties.